Scalar Aharonov-Bohm effect for ultracold atoms

Kenji Shinohara, Takatoshi Aoki, and Atsuo Morinaga
Faculty of Science and Technology, Tokyo University of Science, 2641 Yamazaki, Noda-shi, Chiba 278-8510, Japan
(Received 10 June 2002; published 10 October 2002)

The scalar Aharonov-Bohm effect with a time-dependent magnetic field was investigated for ultracold sodium atoms using the time-domain atom interferometer. The 38 interference fringes with almost the same amplitude verified the nondispersivity of this effect. The measured phase shift as a function of the strength of the applied magnetic field agreed with the predicted one within an accuracy of 3%. With a weak magnetic field orthogonal to the quantization axis, the phase shift was in proportion to the variation of the strength of the resultant magnetic field.

DOI: 10.1103/PhysRevA.66.042106 PACS number(s): 03.65.Vf, 03.75.Dg, 32.60.+i, 39.20.+q

In 1959, Aharonov and Bohm presented their well-known paper on the physical significance of electromagnetic potentials in quantum mechanics and proposed two electron interference experiments to verify the reality of the scalar potential and the vector potential, known as the scalar and the vector Aharonov-Bohm (AB) effects [1]. Subsequently, both effects were extended to neutral particles with a magnetic moment due to the duality of e-μ as reported by Aharonov and Casher [2] and Anandan [3], independently. The vector AB effect has been verified for electrons in an elegant electron holography experiment by Tonomura *et al.* [4] For neutral particles, the first demonstration of the Aharonov-Casher (AC) effect was with slow neutrons by Cimmino *et al.* [5], who used real-space interferometry. This was followed by an excellent spin-space interferometry (i.e. Ramsey-type) experiments with neutral atoms by several groups [6–8]. Recently, Morinaga and co-workers successfully observed the AC phase directly for a relatively short measurement time by developing an atomic polarizing white color interferometer [9].

On the other hand, the scalar AB (SAB) effect, the concept of which is rather simple, has not yet been performed for electrons because of the technical difficulties, but analogous experiments with neutrons have been performed by Allman *et al.* [10] and Badurek *et al.* [11] and with neutral atoms by NicChormaic *et al.* [12]. In those experiments, while a split wave packet of neutral particles remains in the magnetic-field region, a time-dependent homogeneous magnetic field is provided by switching it on and off. Hence there is no force acting on the particle and the phase shift is entirely due to a scalar potential $V=-\boldsymbol{\mu}\cdot\mathbf{B}(t)$. If the initial quantization axis of magnetic moment is parallel to the applied magnetic field, the potential is given by $V=-m_F g_F \mu_B B(t)$, where m_F is the magnetic quantum number of the F state, g_F is the g factor, and μ_B is the Bohr magneton. Thus, the magnetic field $B(t)$ leads to a phase shift of wave packets between the $|F,m_F\rangle$ and the $|F',m_{F'}\rangle$ states,

$$\Delta\varphi_{SAB}=-\frac{\mu_B}{\hbar}(g_{F'}m_{F'}-g_F m_F)\int B(t)dt. \qquad (1)$$

The essential feature of the SAB effect is nondispersivity, which is independent of the velocity of particles. The neutron experiment by Badurek *et al.* demonstrated nondispersivity by observation of phase shifts of up to 60 rad without the loss of contrast [11]. Allman *et al.* showed no difference between the SAB effects for polarized and unpolarized neutron beams [10,13], and confirmed the SAB effect with an accuracy of 6% within a phase shift of $\pm\pi/2$. On the other hand, NicChormaic *et al.* examined the SAB effect for neutral atoms using an atomic Stern-Gerlach interferometer and succeeded in measuring the same fringe period for two different atom velocities, but the size of interference fringes decreased without velocity selection [12]. Müller *et al.* measured the SAB effect for cold atoms with an electric dipole moment in the light-shift potentials using the time-domain atom interferometer [14]. The advantage of using cold atoms is that the interference takes place in a very small volume of space, which facilitates the creation of specially homogeneous interaction potentials. Therefore, several experiments of atomic multiple-beam interferometers using the SAB effect have been demonstrated recently [15–17]. However, obvious verification of the SAB effect using the cold atoms has not yet been reported. Such a time-dependent magnetic field with an arbitrary direction will limit the ultimate accuracy of the frequency standards that utilize the method of atom interferometers.

We have developed a time-domain atom interferometer using a cold sodium atom ensemble in a magneto-optical trap [18]. The cold atom ensemble in the initial ground hyperfine state was excited to another ground hyperfine state by two Raman pulses separated in time and the interference fringe between two wave packets was obtained from the population distribution of atoms in one of the final states. The cold ensemble with a temperature of less than 1 mK still has a thermal velocity, but it drifts over a length of less than 1 mm during the duration of less than 1 ms between the two pulses. We can easily apply a time-dependent homogeneous magnetic field to the entire cold ensemble using a solenoid coil. If we select two states with different magnetic sublevels as two arms of the interferometer, the phase difference between two wave packets can be observed by applying a pulsed magnetic field between two Raman pulses [17]. Therefore, the experimental setup seems to be suitable for verifying the SAB effect.

In this study, we demonstrate an unprecedented nondispersivity using a time-domain atom interferometer. With an

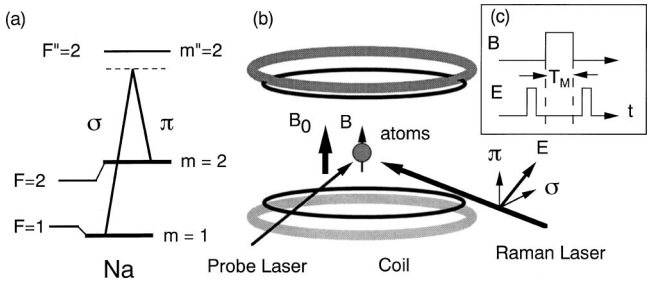

FIG. 1. Experimental scheme for the measurement of the scalar Aharonov-Bohm effect using a time-domain atom interferometer. (a) A partial level scheme of Na with a Raman transition using two polarized photons. (b) Time-domain atom interferometer with magnetic fields. The cold atom ensemble is excited by two Raman pulses and probed by the transition from the $3S_{1/2}$, $F=2$ to $3P_{3/2}$, $F''=3$ state. (c) Timing diagram of the two Raman pulses and a pulsed magnetic field.

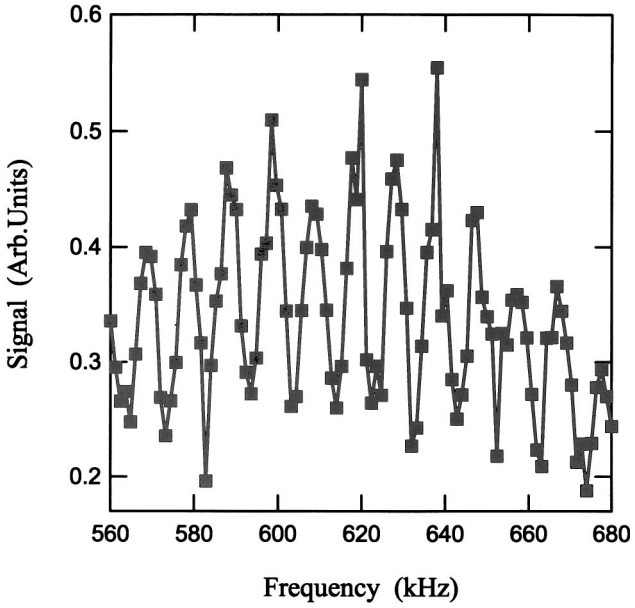

FIG. 2. Ramsey fringes for the transition between the $F=1$, $m_F=1$ to $F'=2$, $m_{F'}=2$ of the $3S_{1/2}$ states under magnetic field. The time separation between two Raman pulses is 100 μs. The resonance frequency is shifted by 620 kHz from the 0-0 transition.

applied magnetic field parallel or orthogonal to the quantization axis, the obtained phase shifts are compared with the predicted one quantitatively in order to verify the scalar Aharonov-Bohm effect.

The time-domain sodium atom interferometer used is almost the same as the previously reported one [18], except that the magnetic substate of atoms was selected under the quantization magnetic field. The experimental setup is shown in Fig. 1. The sodium atom ensemble in the ground $F=2$ state was trapped in the conventional magneto-optical trap. After turning off the quadruple magnetic field, the ensemble was cooled to 200 μK by polarization gradient cooling. After 3 ms, which was the time required for eliminating the quadrupole magnetic field, sodium atoms were initialized perfectly by optical pumping to the $F=1$ state. Then the magnetic field with a strength of B_0 ($\sim$0.2 G) was applied to the atomic ensemble, the quantization axis was defined and the Raman pulse that transits atoms from the $3S_{1/2}$, $F=1$, $m_F=1$ state to the $F'=2$, $m_{F'}=2$ state via $3P_{3/2}$, $F''=2$, $m_{F''}=2$ state was applied.

The frequency of the dye laser was detuned by a frequency of 500 MHz, which is less than the resonance frequency of the transition from $F=1$, $m_F=1$ to $F''=2$, $m_{F''}=2$. The other frequency of the Raman transition was produced through an electro-optic modulator at approximately 1.77 GHz, which corresponds to the hyperfine separation between the $F=1$, $m_F=1$ state and the $F'=2$, $m_{F'}=2$ state. The difference between the two frequencies was tuned exactly to the resonance frequency under the quantization magnetic field. The polarization azimuth of the laser was set to 45° from the quantization axis. Therefore, the Raman transition was generated by the excitation with σ^+ and π polarizations. When the weak magnetic field was applied parallel to the quantization field by a solenoid coil, the resonance peak was shifted further.

The time-domain atom interferometer was produced by two excitations of cold atoms with Raman pulses separated in time. Two Raman pulses with a pulse width of 10 μs and an excitation power of the $\pi/2$ pulse area were applied to the atoms. The pulse separation could be changed to 1 ms, but 200 μs were used in the measurements. Under this condition, Ramsey fringes were generated in the spectrum as detuning of the rf frequency near the resonance, as shown in Fig. 2. The Raman transition from the $F=1$, $m_F=1$ to $F'=2$, $m_{F'}=2$ was shifted by 620 ± 2 KHz from the 0-0 transition at 0.295 G. We calibrated the strength of the applied magnetic field using the measured frequency shift of the central Ramsey or Rabi resonance.

The rf frequency was fixed near the central frequency of resonance and a weak magnetic field of up to 0.1 G was switched on and off with a rise time of 10 μs, during two Raman pulses. After the second Raman pulse was switched off, the probe laser beam that resonates to the $F=2$ state was switched on and the transmittance through the ensemble was measured. At 10 ms interval, these time sequences were repeated and data were accumulated as a function of the strength or the duration of the applied magnetic field.

First, the axis of a weak applied field was set to be parallel to the direction of the quantization axis. A background inhomogeneous magnetic field was removed carefully using compensation solenoid coils. Figure 3 shows two parts of the observed interference fringes as a function of the strength of the pulsed magnetic field with a pulse width of 160 μs. Up to the maximum field of 97 mG, we observed 38 interference fringes corresponding to a phase difference of 240 rad. Moreover, the interference fringes maintain 90% of their initial size during the phase shift of 200 rad. The mean velocity of the cold atoms was 42 cm/s, which corresponds to the de Broglie wavelength of 42 nm. The velocity width is almost of the same order as the mean velocity, so that the coherent length is about 15 nm. However, if the present phase shift is due to the velocity of atoms, the relative displacement between two wave packets will be larger than 1.6 μm, which exceeds the coherent length by two orders of magnitude.

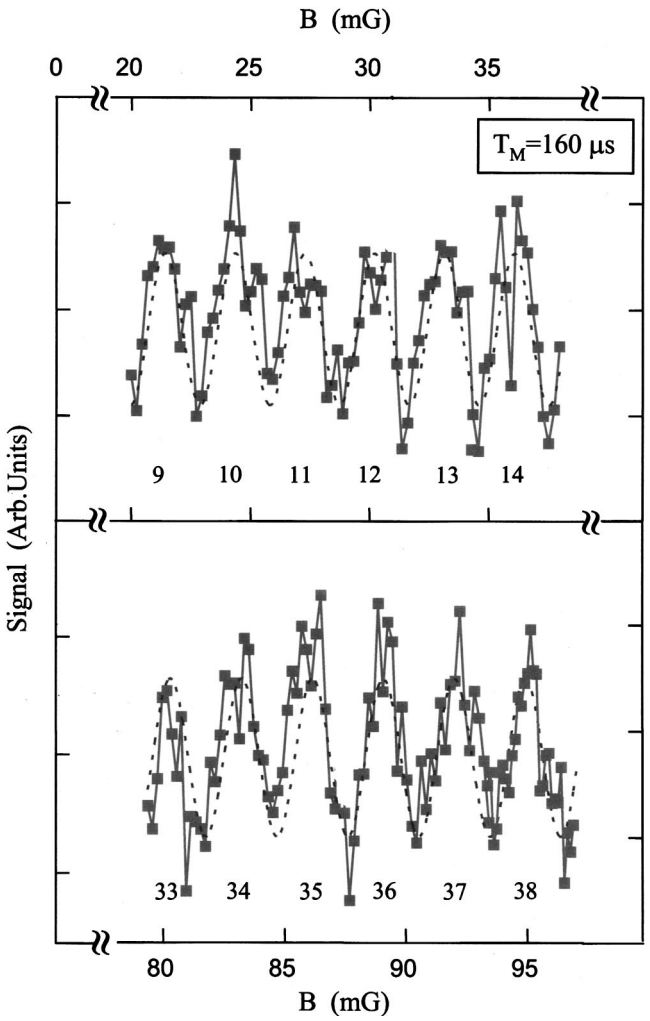

FIG. 3. Examples of the interference fringes due to the scalar Aharonov-Bohm effect observed as a function of the strength of magnetic field up to 97 mG. The time separation between two Raman pulses is 200 μs, while the duration of magnetic field is 160 μs. The figures are consecutively numbered.

This result demonstrates, obviously, the nondispersivity of the SAB effect for the neutral atoms.

If the applied field is rectangular with amplitude B and width T, Eq. (1) becomes

$$\Delta\varphi_{SAB} = -\frac{\mu_B}{\hbar}(g_{F'}m_{F'} - g_F m_F)BT \equiv \alpha BT. \qquad (2)$$

For the present cases, the theoretical value of α is 1.32×10^7 G^{-1} s^{-1}. We deduced the experimental value of α from the measurements of αB by changing the pulse width by ΔT under a certain strength of the applied magnetic field. Then the phase shift during ΔT, $\Delta\varphi_{SAB}$ equals $\alpha B\Delta T$. The measured αB is plotted as a function of the strength of the magnetic field in Fig. 4, together with a straight line with a slope of the theoretical α. The $\alpha_{expt.}$ obtained from the experimental data is $(1.29\pm0.04)\times10^7$ G^{-1} s^{-1}. Therefore we have confirmed the predicted size of the SAB effect within an accuracy of 3%.

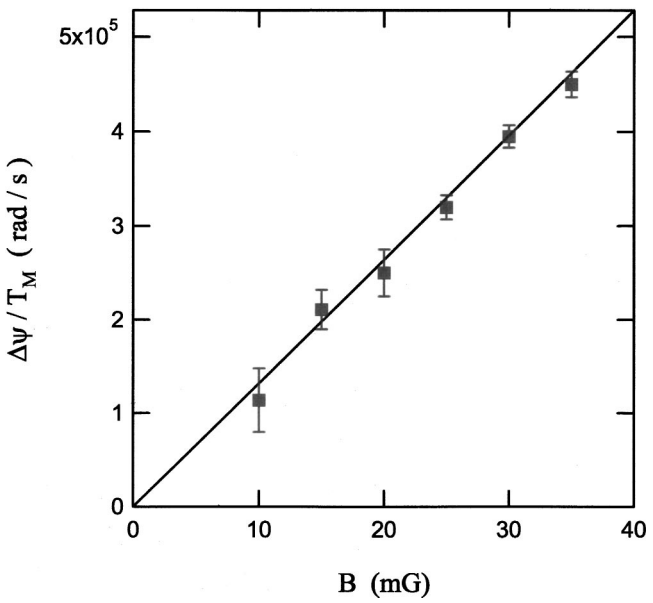

FIG. 4. Ratio of the phase shift to the duration of the pulse as a function of the strength of the applied magnetic field, together with a predicted straight line with a slope of 1.32×10^7 G^{-1} s^{-1}.

The cold atoms expand slowly in all directions within 1 ms after swiching off the trapping laser. The fact that the experimental phase shift was consistent with the theoretical one means that the phase difference does not depend on the direction of atomic motion. Even if the atoms are at rest, the same phase shift occurs.

Finally, the direction of the weak applied field was rotated to be orthogonal to the initial quantization axis. The interference fringes over the same strength of the applied field are shown in Fig. 5. We observe that the phase shift was markedly reduced to less than three fringes, compared with the

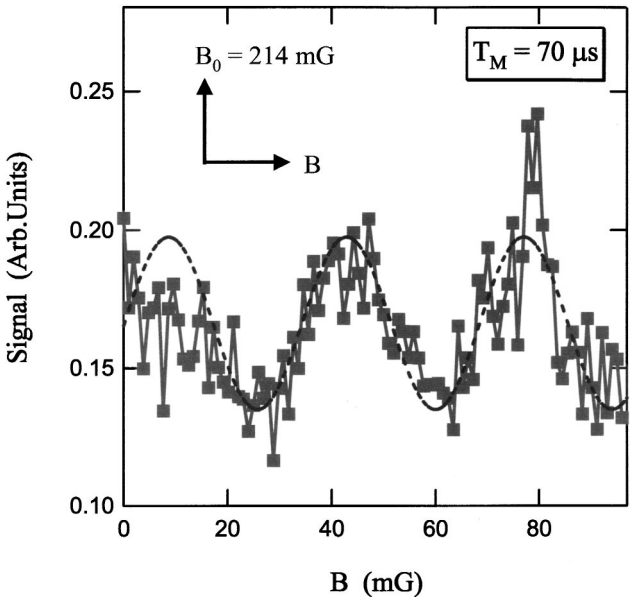

FIG. 5. Interference fringes under the applied magnetic field orthogonal to the initial quantization axis versus the strength of the applied magnetic field with a pulse width of 70 μs.

result of the parallel case obtained for $B=97$ mG and $T=70$ μs. The result can be interpreted as follows. With an orthogonal applied field, the magnetic dipole moment follows adiabatically the direction of the resultant magnetic field, which comprises the quantization field and the relatively small applied field. Therefore the potential depends on the strength of the resultant magnetic field, and the phase between two wave packets changes during a time duration T,

$$\Delta\varphi_{SAB}=\alpha(\sqrt{B_0^2+B^2}-B_0)T. \quad (3)$$

After the applied field is turned off, the magnetic dipole moment returns to the initial quantization direction and resonant atoms to the second Raman pulse, the frequencies of which are same as the first Raman pulse. For the present case, $B_0=214$ mG and $B=97$ mG with a pulse width of 70 μs yield a phase shift of 19 rad, which corresponds to three fringes. The measured phase shift was a little smaller than the predicted value. In the present work, the ratio of the Larmor frequency to the field rotation rate was almost unity, so that some nonadiabatic transitions might be induced as the strength of applied field increased [15]. Thus, the phase shift of atoms in a time-dependent magnetic field is well described by this interpretation.

In conclusion, we demonstrated the phase shift with nondispersivity due to the scalar Aharonov-Bohm effect using a time-domain atom interferometer with a pulsed magnetic field and verified the SAB effect. The time-domain atom interferometer is one promising way to evaluate the frequency standard [19]. Therefore, the SAB effect must be taken into consideration as one of the sources of error. Indeed, the frequency standard normally uses the $m=0$ states, so that the effect will be of second order and hence negligibly small. The authors are aiming to develop a high-finesse atomic multiple-beam interferometer using multiple Raman pulses with multiple magnetic pulse fields [17].

[1] Y. Aharonov and D. Bohm, Phys. Rev. **115**, 485 (1959).
[2] Y. Aharonov and A. Casher, Phys. Rev. Lett. **53**, 319 (1984).
[3] J. Anandan, Phys. Rev. Lett. **48**, 1660 (1982).
[4] A. Tonomura, N. Osakabe, T. Matsuda, T. Kawasaki, J. Endo, S. Yano, and H. Yamada, Phys. Rev. Lett. **56**, 792 (1986).
[5] A. Cimmino, G.I. Opat, A.G. Klein, H. Kaiser, S.A. Werner, M. Arif, and R. Clothier, Phys. Rev. Lett. **63**, 380 (1989).
[6] K. Sangster, E.A. Hinds, S.M. Barnett, and E. Riis, Phys. Rev. Lett. **71**, 3641 (1993).
[7] A. Gorlitz, B. Schuh, and A. Weis, Phys. Rev. A **51**, R4305 (1995).
[8] K. Zeiske, G. Zinner, F. Riehle, and J. Helmcke, Appl. Phys. B: Lasers Opt. **60**, 205 (1995).
[9] S. Yanagimachi, M. Kajiro, M. Machiya, and A. Morinaga, Phys. Rev. A **65**, 042104 (2002).
[10] B.E. Allman, A. Cimmino, G.I. Opat, A.G. Klein, H. Kaiser, and S.A. Werner, Phys. Rev. Lett. **68**, 2409 (1992).
[11] G. Badurek, H. Weinfurter, R. Gähler, A. Kollmar, S. Wehinger, and A. Zeilinger, Phys. Rev. Lett. **71**, 307 (1993).
[12] S. NicChormaic, Ch. Miniatura, O. Gorceix, B.V. Lesengo, J. Robert, S. Feron, V. Leorent, J. Reinhardt, J. Baudon, and K. Rubin, Phys. Rev. Lett. **72**, 1 (1994).
[13] B.E. Allman, W.-T. Lee, O.I. Motrunich, and S.A. Werner, Phys. Rev. A **60**, 4272 (1999).
[14] J.H. Müller, D. Bettermann, V. Rieger, K. Sengstock, U. Sterr, and W. Ertmer, Appl. Phys. B: Lasers Opt. **60**, 199 (1995).
[15] É. Maréchal, R. Long, J.- L. Bossennec, R. Barbé, J.-C. Keller, and O. Gorceix, Phys. Rev. A **60**, 3197 (1999).
[16] M. Mei, T.W. Hänsch, and M. Weitz, Phys. Rev. A **61**, 020101(R) (2000).
[17] K. Shinohara, T. Aoki, and A. Morinaga, in *Proceedings of ISQM-Tokyo '01*, edited by by Y.A. Ono and K. Fujikawa (World Scientific, Singapore, in press).
[18] T. Aoki, K. Shinohara, and A. Morinaga, Phys. Rev. A **63**, 063611 (2001).
[19] T. Trebst, T. Binnewies, J. Helmcke, and F. Riehle, IEEE Trans. Instrum. Meas. **50**, 535 (2001).